Constrained Multivariable Optimization of Transmission Lines With General Topologies*

Rohini Gupta† and Lawrence T. Pileggi‡
Department of Electrical and Computer Engineering
The University of Texas at Austin
Austin, TX 78712

Abstract

The design of system level interconnects to meet signal integrity objectives is a challenging problem. This paper formulates the transmission line synthesis problem as a constrained multi-dimensional optimization of the complete net, taking into account factors like loading conditions on the line, loss in the line and rise-time of the input signal. Different design variables such as width or resistivity of the interconnect, resistive source or far-end termination, etc. can all be considered concurrently.

The termination metric is based upon forcing the impulse response waveform to be symmetric using the first three exact moments of the distributed system. An efficient means to trade-off between signal rise-time and ringing is presented and no time-domain simulations are needed. Several examples are presented to demonstrate the efficacy of the proposed methodology.

1: Introduction

Increasing switching speeds and complexity of VLSI circuits is taking the task of system level interconnect design from the realm of purely "a designer's intuition" to that which requires the aid of a CAD tool. Signal integrity is becoming a significant factor in determining the reliability and performance of an electronic system, and enormous resources are being harnessed to analyze and ensure that signal integrity objectives are met. For high-performance systems, designers are beginning to promote the task of system level interconnect design from a mere trouble-shooting problem to a front-end design and synthesis objective.

In previous work on transmission line synthesis, interconnect models have been used to obtain a simplified pole-zero description of the circuit behavior[3,15]. In [5], a distributed interconnect model is used for self-damping lossy transmission lines on MCMs, but this method and the lumped RLC approximations are limited to pin-to-pin nets and cannot account for driver rise-time or loading conditions on the line effectively. Since transmission line effects dominate when the rise-time, t_r, is much smaller than the time-of-flight on the line, rise-time is an important parameter affecting transmission line behavior. In [17], a reduced order two-pole approximation is obtained for the transfer function after extracting the high-frequency time-of-flight of the transmission line. This preprocessing step of extracting the time-of-flight[17] and generating an effective two-pole representation taking into account the effect of "off-path" loads[19,21] for a general transmission line topology presents a costly overhead for a design automation tool.

Moment based techniques for optimal termination have been presented in [7,11] to efficiently account for loading conditions on the line, loss in the line and the input signal rise-time. The symbolic treatment in [7] offers an efficient and effective technique for pin-to-pin transmission line nets. This paper generalizes these moment-based metrics to consider arbitrary transmission line tree structures, and formulates the design objective as a nonlinear constrained optimization problem.

Moments are used as metrics of the distributed transmission line model that characterize the signal behavior such that synthesis is feasible in the frequency domain without resorting to any preprocessing steps or time-domain simulations[8,11]. This allows the integration of different design variables such as width, length of the line, resistive source or far-end termination, etc., into a common

* This work was supported in part by the Semiconductor Research Corporation under contract 95-DJ-343 and the National Science Foundation under contract MIP-9157263.
† Rohini Gupta is now with AT&T Bell Laboratories, Allentown PA 18103.
‡ Formerly Lawrence T. Pillage. As of January 1996, he will be with Carnegie Mellon University, Dept. of ECE, Pittsburgh, PA 15213.

design optimization tool. Along with delay metrics presented in [11] for a properly terminated transmission line net, this constitutes a powerful technique for transmission line synthesis. Several examples and results are presented to demonstrate the efficacy of the proposed methodology and optimization framework.

2: The Termination Objective

The transmission line is a medium for transfer of electrical signals in a VLSI system and a perfect transmission medium would be one that transmits the input signal undistorted. At a particular node k of a transmission line tree, let the output response be given by $v_{o,k}(t) = h_k(t) * v_i(t)$, where $h_k(t)$ is the impulse response at that node, $v_i(t)$ is the input signal and * is the convolution operator. This paper formulates the termination objective as a design problem where $h_k(t)$ is designed to transmit $v_i(t)$ with minimum distortion.

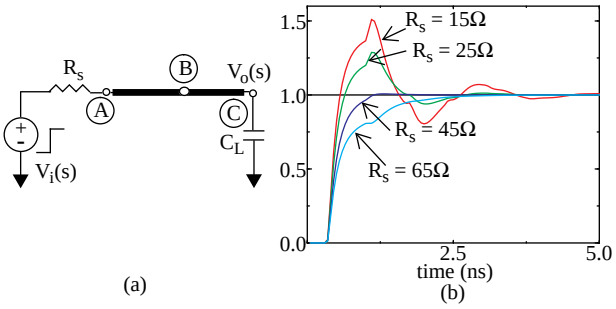

FIGURE 1: (a) A source-terminated transmission line. (b) Trade-off between rise-time and ringing. R=2Ω/cm, L=3.35nH/cm, C=1.34pF/cm, C_L=3pF, Z_0=50Ω and d=5cm.

Since excessive settling time effectively increases delay, both under-damping and over-damping adversely impact delay, as shown in Fig.1(b) for the circuit in Fig.1(a). A designer generally wants to minimize ringing while maximizing the signal slope (minimizing rise-time). Moments of the impulse response $h_k(t)$ can be used to achieve this objective without computationally expensive time-domain simulations.

2.1: Moments of the Impulse Response

Under conditions of analyticity, the transfer function of a system can be expanded into its Maclaurin series:

$$H(s) = \int_0^\infty e^{-st} h(t)\,dt = \sum_{k=0}^{\infty} \frac{(-1)^k}{k!} m_k \qquad (1)$$

where m_k is the k-th moment of the impulse response:

$$m_k = \int_0^\infty t^k h(t)\,dt \qquad (2)$$

For the simple source-terminated transmission line in Fig.1(a), the transfer function is [8]:

$$\begin{aligned} H(s) &= \frac{V_o(s)}{V_i(s)} \\ &= 1/\,[\,sC_L\,(R_s \cosh(\gamma d) + Z_0 \sinh(\gamma d)) + \\ &\qquad (R_s/Z_0)\sinh(\gamma d) + \cosh(\gamma d)\,] \end{aligned} \qquad (3)$$

where, $\gamma = \sqrt{(R+sL)(sC)}$ is the *propagation function* and $Z_0 = \sqrt{(R+sL)/(sC)}$ is the *characteristic impedance* of the line. R, L and C are the resistance, inductance and capacitance of the transmission line per unit length respectively, d is the length of the line and the series resistance, $R_s = R_{dr} + R_{ter}$, where R_{dr} is the driver resistance and R_{ter} the additional termination resistance. The dielectric loss, G, is assumed to be negligibly small. From (1) and (3), the transfer function moments for the transmission line system can be obtained as a function of R_s [7]. The driver resistance R_{dr} is assumed to be linear in this paper, since driver linearization schemes can be applied without loss of generality[9].

From the definition of moments in (2), the *mean* of the impulse response is given by[4,8]:

$$\eta = \frac{\int_0^\infty t h(t)\,dt}{\int_0^\infty h(t)\,dt} = \frac{m_1}{m_0} \qquad (4)$$

When the dc gain of the system is unity, $m_0 = 1$ and the mean, $\eta = m_1$. *Central moments* of the impulse response are defined as moments about the *mean* and are given by[8]:

$$\mu_k = \int_0^\infty (t-\eta)^k h(t)\,dt \qquad (5)$$

In terms of the circuit moments in (2), the first few central moments can be expressed as follows:

$$\begin{aligned} \mu_0 &= m_0 \\ \mu_1 &= 0 \\ \mu_2 &= m_2 - \frac{m_1^2}{m_0} \\ \mu_3 &= m_3 - \frac{3m_1m_2}{m_0} + 2\frac{m_1^3}{m_0^2} \\ &\textit{and so on ...} \end{aligned} \qquad (6)$$

The second central moment μ_2 is a function of the second power of $(t-\eta)$ in (5) and provides a measure of the spread or *dispersion* of the function $h(t)$. Similarly, the third central moment, μ_3, is a function of an odd power of $(t-\eta)$ and is a measure of the *asymmetry* of $h(t)$ [4,8]. In the following section, these central moments and their properties are used to obtain a metric for optimal termination of a transmission line.

2.2: A Metric for Optimal Termination

For an unloaded lossless transmission line driven by a step input as shown in Fig.2(a), it is well known that the optimal termination resistance is $R_s = Z_0$ [1,7]. With this termination, for a lossless line (from equation (3) with $R = 0$, $C_L = 0$ and $V_i(s) = 1/s$),

$$V_o(s) = \frac{1}{(R_s/Z_0)\sinh(\gamma d) + \cosh(\gamma d)} \cdot \frac{1}{s} = e^{-\gamma d} \cdot \frac{1}{s} \tag{7}$$

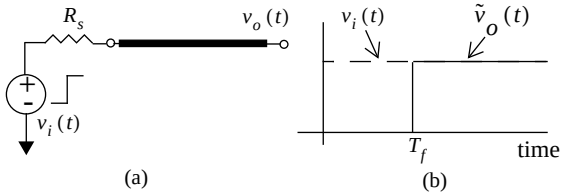

FIGURE 2: (a) A perfect lossless, unloaded transmission line. Time-of-flight, $T_f = \sqrt{LC}d$, where d is the length of the line. (b) Input $v_i(t)$ and ideal output response $\tilde{v}_o(t)$.

Thus, the ideal signal under optimal termination is the input step delayed by the time-of-flight along the line given by $T_f = \sqrt{LC}d$ which is also the mean of the impulse response for this system[8]. For this ideal response, it can be verified that the second and third central moments about the mean $\eta = \sqrt{LC}d$ are exactly zero[8,10]. Now, μ_2 and μ_3 for an unloaded lossless transmission line are given by

$$\mu_2 = -CLd^2 + R_s^2C^2d^2$$
$$\mu_3 = -2R_sC^2Ld^3 + 2C^3d^3R_s^3 \tag{8}$$

Symbolically solving $\mu_2 = 0$ for R_s yields two roots (as shown in Fig.3(a)):

$$\sqrt{\frac{L}{C}}, -\sqrt{\frac{L}{C}} \tag{9}$$

and solving $\mu_3 = 0$ yields three roots (Fig.3(b)):

$$0, \sqrt{\frac{L}{C}}, -\sqrt{\frac{L}{C}} \tag{10}$$

The positive root provides the solution, $R_s = \sqrt{L/C} = Z_0$.

Thus, the ideal impulse response for a lossless transmission line is symmetric and localized (zero dispersion) about its mean. And conversely, forcing the impulse response to be symmetric and localized about the mean ensures critical damping.

Lossy lines, however, exhibit the phenomenon of "dispersion" which is due to the dependence of the phase velocity of a propagating wave on the frequency of the signal component[16]. Consequently, for a signal comprising of a band of frequencies, the different frequency components do not maintain the same phase relationships as they propagate down the line. Due to this inherent property of dispersion of a lossy transmission line, μ_2, being a measure of dispersion, cannot vanish simultaneously along with μ_3 for a lossy transmission line.

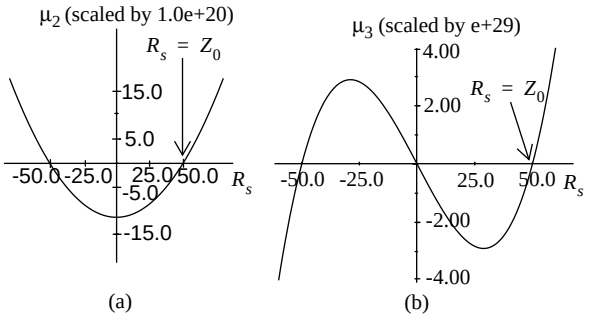

FIGURE 3: (a) μ_2 vs. R_s and (b) μ_3 vs. R_s for a lossless, unloaded transmission line. $Z_0 = 50\Omega$.

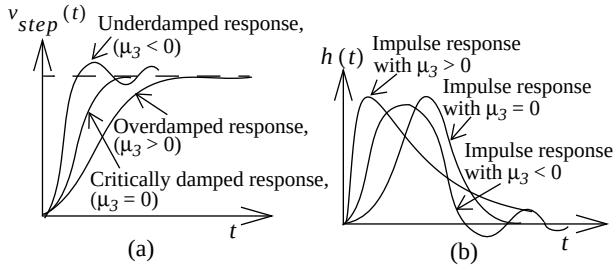

FIGURE 4: (a) Underdamped, critically damped and overdamped step responses. (b) Impulse responses with positive, zero and negative μ_3's corresponding to overdamping, critical damping and underdamping, respectively.

For a positive function $h(t)$, since the third central moment μ_3 is known to be a measure of the *asymmetry* of the function, $\mu_3 > 0$ represents a positively skewed function with a long right tail, as shown in Fig.4(b), and corresponds to an overdamped signal (Fig.4(a)). For a transmission line system, when the response is underdamped, there is some overshoot/undershoot, and so, for the impulse response shown in Fig.4(b), $\mu_3 < 0$. The third central moment from equation (5) can be rewritten as,

$$\mu_3 = \underbrace{\int_0^{\mu} (t-\mu)^3 h(t)\,dt}_{\mu_3^-} + \underbrace{\int_{\mu}^{\infty} (t-\mu)^3 h(t)\,dt}_{\mu_3^+} \tag{11}$$

so that for $h(t) \geq 0$, $\mu_3^- = \mu_3^+ \Rightarrow \mu_3 = 0$, which corresponds to a critically damped system.

Thus, for a lossy transmission line, the objective is to design the impulse response to be localized and symmetric about its mean. And since μ_3 is a measure of asymmetry and hence ringing, as discussed above, $\mu_3 = 0$ with minimum μ_2 is proposed to be the condition for optimal termi-

nation for a lossy transmission line. However, in order to minimize ringing while maximizing the signal slope, we discuss in Section 4 how a ringing versus rise-time tradeoff can be made using the second central moment, μ_2.

2.3: Reflected Wave Switching

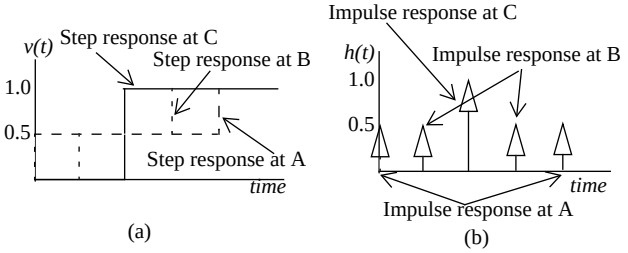

FIGURE 5: (a) Reflected wave switching. (b) Impulse responses at nodes A, B and C.

Referring to Fig.1(a), for the ideal case of a step input, lossless line and small capacitive load, node C is switched by the incident wave and the ideal response is as shown in Fig.5(a). For this source terminated transmission line, the incident wave switches the points A and B along the line to half the final value, and then the reflected wave completes the switching, as shown in Fig.5(a). This type of switching—called reflected wave switching—occurs when a transmission line net in a daisy-chain configuration is source terminated. For a system with zero initial state, the derivative of the step response $v_o(t) = h(t) * v_i(t)$ gives the impulse response[14], and Fig.5(b) shows the impulse responses at nodes A, B and C, respectively.

The common feature among the responses at A, B and C in Fig.5(b) is that each of these is a symmetric function. Nodes A and B are switched by the reflected wave and C is switched by the incident wave, but for ideal switching behavior, each of these has a symmetric impulse response. We use this property of symmetry to provide a cost function for optimal termination in terms of only the first four moments of the transfer function. *Thus, for both incident and reflected wave switching, in order to minimize ringing, the objective is to force the response to be a symmetric function, i.e.* $\mu_3 = 0$.

3: The Optimization Framework

3.1: The Objective Function

With the objective function for optimal termination defined as $\mu_3 = 0$, for N observation points on a transmission line net,

$$\Phi = \left[\mu_3^{(1)} \mu_3^{(2)} \mu_3^{(3)} \mu_3^{(4)} \ldots \mu_3^{(N)}\right]^T \tag{12}$$

where $i = 1 \ldots N$ are the points of interest, so that $\Phi \in \Re^N$. $\mu_3^{(i)}$ is the third central moment at node i and is a function of the variable element vector,

$$\mathbf{x} = [x_1\ x_2\ x_3\ \ldots\ x_K]^T \tag{13}$$

where $\mathbf{x} \in \Re^K$. The variable element x_j may be a termination resistor, width of the transmission line, length of the line, or any other parameter. The cost function $P(\mathbf{x})$ is related to the Euclidean norm of the vector Φ:

$$P(\mathbf{x}) = (\|\Phi\|_2)^2 = \sum_{i=1}^{N} \left(\mu_3^{(i)}\right)^2 \tag{14}$$

and the constraints on the problem are in the form of bounds on the variables x_j so that, $\forall j, x_j \geq l_j$. Upper bounds can also be incorporated into this form since $x_j \leq u_j \Rightarrow -x_j \geq -u_j$. For a termination resistor, the lower bound is $l_j = 0$, for wire-width variation, $l_j = w_{min}$, where w_{min} is a minimum geometry constraint or a delay constraint[9], and so on. The width constraint w_{min} can be expressed as a function of other design factors such as electromigration and signal cross-talk.

3.2: Minimization Subject to Bounds Constraint

The objective of the optimization problem is:

$$\begin{aligned} &\textit{minimize} \quad P(\mathbf{x}) \\ &\textit{subject to} \quad \mathbf{A}\mathbf{x} \geq \mathbf{l} \end{aligned} \tag{15}$$

where the rows of $\mathbf{A}$ are signed rows of the identity matrix and a bound constraint i is considered "active" when $x_i = l_i$. The problem in (15) defines a nonlinear optimization task with linear constraints. We follow a quasi-Newton approach to minimize $P(\mathbf{x})$ and exploit the knowledge that the constraints are in the form of bounds. This allows us to perform unconstrained minimization within a working set that is constituted of the "inactive" or free variables, as follows.

At iteration k, if t_k variables are fixed on their respective bounds, then the vector $\mathbf{x}_k$ can be partitioned into its free components $\mathbf{x}_{FR}$ and its fixed components $\mathbf{x}_{FX}$. The rows of the t_k-rank matrix $\hat{\mathbf{A}}_k$ are a selection of the rows of $\mathbf{A}$ corresponding to the fixed variables. $\mathbf{x}_{FR}$ is called the *working set* of the problem and the corresponding gradient vector is Λ_{FR}. The minimization of $P(\mathbf{x})$ follows the search direction determined by the negative gradient of the cost function with respect to the working set. The search direction will be zero in components corresponding to the fixed variables.

In a quasi-Newton approach, the search vector $\mathbf{p}_{FR}$ is given by[6,12]:

$$\mathbf{B}_{FR}\mathbf{p}_{FR} = -\Lambda_{FR} \tag{16}$$

where $\mathbf{B}_{FR}$ denotes the $K - t_k$ dimensional approximation

of the Hessian matrix with respect to the free variables (from (13), $\mathbf{x}$ is of dimension K). Changes in the working set simply involves fixing a variable on a bound when a constraint is added, and freeing a variable from its bound if its constraint is deleted. Since Lagrange multipliers are associated only with active constraints, for the constraints in the form of bounds they are simply given by the signed components of the gradient vector corresponding to the given fixed variable. If the j-th fixed variable in $\hat{\mathbf{A}}_k$ is x_i such that $x_i = l_i$, then $\lambda_j = \Lambda_i$ [8].The solution is reached when the Kuhn-Tucker conditions are satisfied[6] and one of the conditions for optimality requires that $\forall j, \lambda_j > 0$.

Initializing the variable set $\mathbf{x}$ such that the vector $\Phi > \mathbf{0}$ (from equation (12)), i.e. $\forall i, \mu_3^{(i)} > 0$, the unconstrained search direction can be obtained using any gradient based technique[12]. (For instance, in Fig.3(b), μ_3 is shown as a function of R_s for a simple lossless transmission line. Clearly, initializing R_s so that $\mu_3 > 0$ ensures that we find the root at $R_s = Z_0$.) We have chosen the quasi-Newton approach mainly due to the "smoothness" of our cost function surface and for its superlinear convergence property[6].

3.3: Moment Computation and Sensitivities

In order to evaluate the cost function and sensitivities, the optimization procedure described above requires an efficient method to calculate the exact moments m_0 through m_3 at each node of interest in a transmission line tree. Circuit moments have been widely used for interconnect analysis and several moment models have been proposed[14]. For a tree topology, the moment model proposed in [20] offers a computational complexity of $O(M)$, where M is the number of nodes in the transmission line tree. Cost function sensitivities can then be calculated efficiently using perturbation and finite-differencing or by adjoint sensitivity techniques[6,10,14].

4: Controlling Response Rise-Time

4.1: Ringing versus Rise-time Trade-Off

In Section 2, the objective of optimal termination was stated as minimizing ringing while maximizing the response signal slope. The objective function in Section 3 aims to minimize ringing by minimizing μ_3 at each node of interest.

For a positive impulse response function, as shown in Fig.4(b), the second central moment μ_2 is a measure of the spread or *dispersion* of the function[4]. Reducing μ_2 (within the constraint that $\mu_2 \geq 0$) reduces the spread of the function and hence results in an output response with a higher transition rate, thereby providing an efficient means to trade-off between rise-time and ringing. For M leaf-nodes in a transmission line tree,

$$\Psi = \left[\mu_2^{(1)} \mu_2^{(2)} \mu_2^{(3)} \mu_2^{(4)} \ldots \mu_2^{(M)}\right]^T \tag{17}$$

so that $\Psi \in \Re^M$ and $\mu_2^{(j)}$ is a function of the variable element vector $\mathbf{x}$ (from equation (13)). Note from Fig.5(b) that the spread, and hence μ_2, for non-leaf nodes A and B depend on their physical positions w.r.t. to node C during reflected wave switching and not solely on the signal transition rate. Thus, we do not formulate the cost function to minimize μ_2 at these nodes. The cost function to maximize the slope of the response signal $Q(\mathbf{x})$ is related to the Euclidean norm of the vector Ψ in (17):

$$Q(\mathbf{x}) = (\|\Psi\|_2)^2 = \sum_{i=1}^{M} \left(\mu_2^{(i)}\right)^2 \tag{18}$$

Thus, to obtain a signal with minimum ringing and maximum slope, $R(\mathbf{x}) = P(\mathbf{x}) + \xi Q(\mathbf{x})$ can be minimized, where ξ is a weighting factor to trade-off between rise-time and ringing. Alternatively, we minimize $P(\mathbf{x})$ and then use the rise-time of the input-signal to minimize $Q(\mathbf{x})$, as discussed below.

4.2: Input Signal Rise-Time Effects

Transmission lines are never driven by step signals. In [9], the nonlinear drivers are modeled by Thevenin equivalents with a ramp voltage input, $v_i(t)$, or

$$V_i(s) = \frac{1 - e^{-t_r s}}{s^2 t_r} \tag{19}$$

where t_r is the rise-time of the voltage input signal. It is well known that transmission line phenomenon for an interconnect becomes insignificant when $t_r > 2.5 \cdot T_f$, where T_f is the time-of-flight on the line, and the line can be modeled as a lumped circuit[1]. Moreover, the line acts as a lumped capacitor when $t_r > 5 \cdot T_f$. Thus, termination requirements for a transmission line need to also account for the frequency content of the input signal[7]. The bandlimitedness of the input signal can be used as a design variable for termination using programmable drivers where rise-time might be controlled. For a saturated ramp given by (19), the central moments are of the form:

$$\mu_1 = \frac{1}{2} t_r \qquad \mu_2 = \frac{1}{12} t_r^2 \qquad \mu_3 = 0 \tag{20}$$

Thus, for $t_r \neq 0$, the "dispersion" of the output response is affected by the rise-time of the input signal (where, $V_o(s) = H(s) V_i(s)$), as shown in Fig.6(b) for a simple

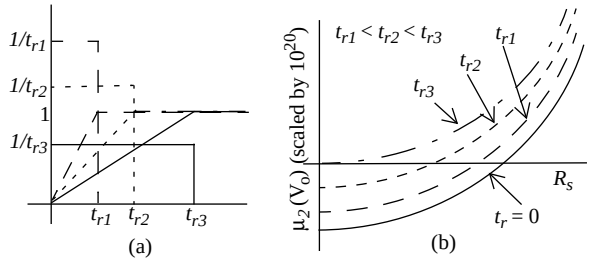

FIGURE 6: (a) Saturated ramp inputs with $t_{r1} < t_{r2} < t_{r3}$. (b) μ_2 as a function of termination resistance R_s for a simple transmission line as in Fig.1(a) with different input signal rise-times, t_r.

transmission line as in Fig.1(a). It can be demonstrated that when $m_0 = 1$ for the impulse response, the central moments add under convolution[8,10]. As the rise-time increases, minimization of $\mu_2(V_o)$ yields a smaller value of the termination resistance R_s. In Fig.6(b), note that for $t_r = t_{r3}$, $\mu_2(V_o)$ is minimized at $R_s = 0$, i.e. the line is self-terminated with rise time t_{r3}. We shall illustrate this effect in Section 5.4 using an example.

5: Synthesis of General Transmission line Net Topologies

In this section, we discuss different transmission line net topologies and optimize selected termination techniques[8,10].

5.1: Star topology

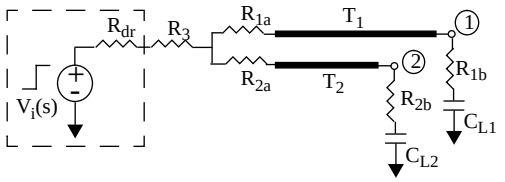

FIGURE 7: A Transmission line star topology. R=1Ω/cm, L=3.35nH/cm, C=1.34pF/cm, Z_0=50Ω, d_1=5cm, d_2=1.25cm, t_r=50ps. R_{dr}=10Ω is the driver resistance. R_{1a} and R_{2a} represent source termination and R_{1b} and R_{2b} far end ac termination.

The star topology shown in Fig.7 is the preferable choice when an interconnect skew between loads is undesirable, such as the case of a clock distribution network[2]. In Fig.7, when $d_1 = d_2$ and $C_{L1} = C_{L2}$, then $R_1 = R_2 = 0$ and the net can be terminated using only one resistor R_3, the value of which can be obtained using the optimization procedure described in Section 3. In general, however, optimizing only R_3 cannot result in a properly terminated signal at both nodes 1 and 2, and so, $R_3 = 0$, and R_1 and R_2 are *simultaneously* optimized. For this topology, we present two types of termination — source termination and far-end ac termination. For source termination, in Fig.7, $R_{1b} = R_{2b} = 0$ and for ac termination,

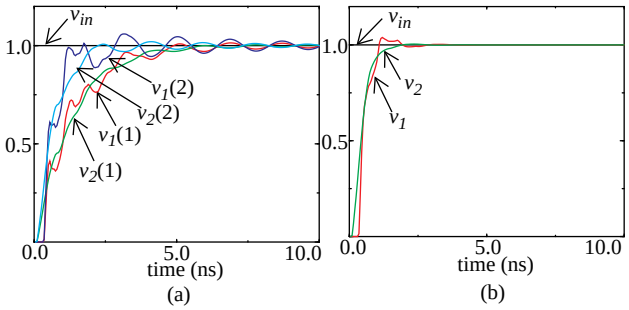

FIGURE 8: Time domain waveforms for source termination with C_{L1}= 3pF and C_{L2}=15pF. (a) $R_1 = R_2 = 0$. $v_1(1)$, $v_2(1)$ show responses at nodes 1 and 2 with $R_3 = 37\ \Omega$ (optimizing μ_3 at node 1), and $v_1(2)$, $v_2(2)$ show responses at nodes 1 and 2 with $R_3 = 15\ \Omega$ (optimizing μ_3 at node 2). (b) $R_3 = 0$, $R_{1a} = 22.5\ \Omega$ and $R_{2a} = 10\ \Omega$ (such that μ_3 are nodes 1 and 2 are simultaneously optimized).

$R_{1a} = R_{2a} = 0$. The time-domain waveforms are shown in Fig.8 and Fig.9. For source termination, the result obtained by minimizing μ_3 at nodes 1 and 2 separately is contrasted in Fig.8(a) against the simultaneous optimization of the termination resistors R_{1a} and R_{2a} in Fig.8(b).

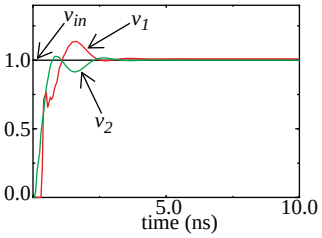

FIGURE 9: Time domain waveforms for far-end ac termination. C_{L1}= 10pF and C_{L2}=15pF. $R_3 = 0$, $R_{1b} = 50\Omega$ and $R_{2b} = 5\Omega$ (such that μ_3 at nodes 1 and 2 are simultaneously optimized).

5.2: Daisy Chain Topology

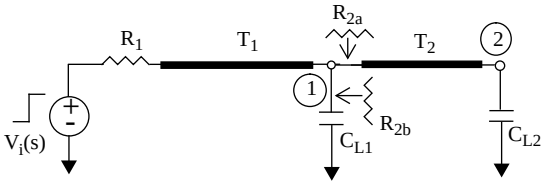

FIGURE 10: Daisy chain connection. R_{2a} represents series termination and R_{2b} represents ac termination. R=0.01Ω/cm, L=3.35nH/cm, C=1.34pF/cm, Z_0=50Ω, d_1=5cm, d_2=5cm, t_r=50ps.

Due to advantages of routing with minimal space requirement, the daisy chain (or multi-drop) configuration as shown in Fig.10 is a popular topology. The behavior is that of a pin-to-pin transmission line if the loads along the line are "small" compared with the line capacitance and the net can be terminated with one resistance R_1 as shown in Fig.10. The propagating signal experiences a discontinuity proportional to the capacitive load since the load pre-

sents an admittance $Y_{C_L} = j\omega C_L$, and so, the propagating signal "dips" in proportion to Y_{C_L} when it sees the capacitive load. In general, the net cannot be properly terminated with only one termination resistance. The number of termination components required is equal to the number of discontinuities, and these should be optimized simultaneously. Here, we show results for both series and ac termination.

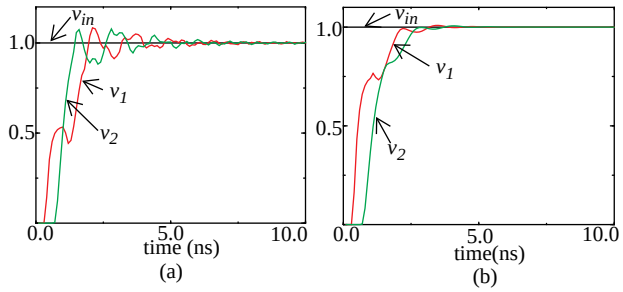

FIGURE 11: Series termination $R_{2b} = 0$. Time domain waveforms for C_{L1}= 5pF and C_{L2}=5pF. (a) $R_{2a} = 0$ and $R_1 = 43\ \Omega$ (optimizing μ_3 at nodes 1 and 2). (b) Series termination with $R_1 = 34\ \Omega$ and $R_{2a} = 38\ \Omega$ (such that μ_3 at nodes 1 and 2 are simultaneously minimized).

The series termination method uses R_{2a} as shown in Fig.10. to present a higher effective impedance in T_2 such that C_{L1} gets charged higher before the wave propagates forward. As shown in Fig.11(b), the noise level is controlled when R_1 and R_{1a} are optimized together. But since this method uses series resistors, it should be used for a smaller number of loads along the net. The use of ac termination has been described earlier in [7]. For a fast-rising signal traveling along the line, C_{L1} acts like a short circuit to ground. When optimized, R_{2b} is the impedance that the signal sees to ground and its distortion is controlled. The value of R_{2b} depends on C_{L1} and other line parameters. Fig.12(b) shows the time-domain waveforms for the example in Fig.10 with ac termination.

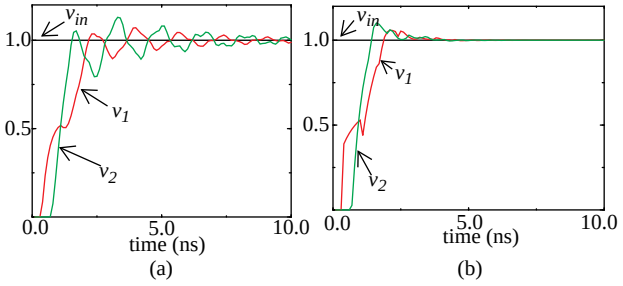

FIGURE 12: ac termination $R_{2a} = 0$. Time domain waveforms for C_{L1}= 10pF and C_{L2}=5pF. (a) $R_{2b} = 0$ and $R_1 = 40\ \Omega$ (optimizing μ_3 at nodes 1 and 2). (b) ac termination with $R_1 = 30\ \Omega$ and $R_{2b} = 37.5\ \Omega$ (such that μ_3 at nodes 1 and 2 are simultaneously minimized).

5.3: Termination Using Wire-Width Variation

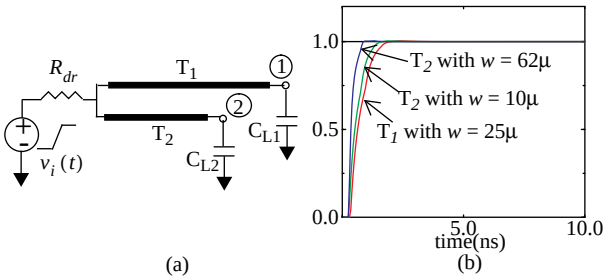

FIGURE 13: Termination via wire-width variation. d_1=5cm, d_2=4cm, t_r=50ps. C_{L1}= 10pF, C_{L2}=5pF, R_{dr}=13.5Ω. With w=25µm, R_1=6Ω/cm, L_1=2.08nH/cm, C_1=1.85pF/cm. With w=10µm, R_2=15Ω/cm, L_2=3.33nH/cm, C_2=1.15pF/cm.

When the exact value of the termination resistance, R_{ter}, is not readily available, we can select the closest $\hat{R}_{ter}$ from the set of available resistor values, and then complete the termination by wire-width optimization. The resistance, inductance and capacitance of the interconnect are functions of the interconnect width, w, and to a first order,

$$R(w) \propto \frac{1}{w} \qquad L(w) \propto \frac{1}{w} \qquad C(w) \propto w \tag{21}$$

where, the exact relations for $R(w)$, $L(w)$ and $C(w)$ are obtained from a parameter extraction model[18]. For example, for the microstrip lines on an MCM in Fig.13(a), with a nominal width of 25µm, the line T_1 with load $C_L = 10\ pF$ is self-terminated with a driver resistance of 13.5Ω. This, however, leaves the line T_2 with a load of $5\ pF$ underdamped. By varying the width of T_2 to 10µm optimally terminates it, as shown in Fig.13(b). The line parameters as a function of line-width are given by:

$$\begin{aligned} R(\Omega/cm) &= 150/w \\ L(nH/cm) &= 1/(0.012w + 0.18) \\ C(pF/cm) &= 0.047w + 0.68 \end{aligned} \tag{22}$$

where w is the width in microns[18]. It is interesting to note that for a lossy transmission line the solution is not unique and depends on the relations in (22). The alternate solution for T_2 is a line width of 62µm. This can be explained as follows: With $R_{dr} = 13.5\Omega$, reducing the width of T_2 increases Z_0, but also increases the total line resistance such that a width of 10µm self-terminates it. On the other hand, increasing w decreases line resistance along with Z_0 such that for a width of 62µm, the driver resistance terminates the line! The choice between the two solutions of 10µm and 62µm will have to be based on factors of power, delay and manufacturability[9].

5.4: Termination Using Rise-time Variation

A typical application for self-termination by varying the rise-time of the driver is for a net where a short trans-

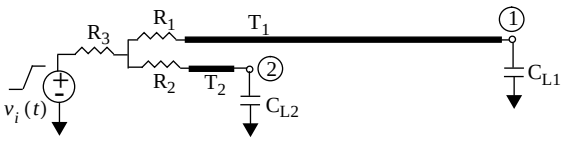

FIGURE 14: A short stub T_2. R_2 can be dispensed with if the rise-time of V_i is a variable parameter. R=2Ω/cm, L=3.35nH/cm, C=1.34pF/cm, Z_0=50Ω, d_1=5cm, d_2=0.5cm, C_{L1}=5pF, C_{L2}=10pF.

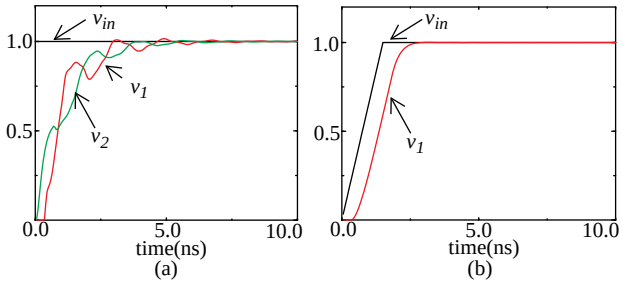

FIGURE 15: (a) Termination using $R_3 = 44\ \Omega$. $R_1 = R_2 = 0$ and $t_r = 50\ ps$. (b) Termination using $R_1 = 44\ \Omega$ (such that μ_3 is minimized) and $t_r = 1.5\ ns$. $R_2 = R_3 = 0$.

mission line stub is present as in Fig.14. By degrading the input signal rise-time, as discussed in Section 4, μ_2 at node 2 results in the self-termination of the line T_2 with a rise-time of 1.5ns, and then R_1 can be used to terminate T_1, as in Fig.15(b). Fig.15(a) shows the time-domain waveforms at nodes 1 and 2 when R_3 is used to terminate the system for a step input and $R_1 = R_2 = 0$.

6: Conclusions

This paper has presented a methodology for optimal termination of a general transmission line tree using only the first few moments of the impulse response of the system, and without any time-domain simulations. The metric accounts for factors like loading conditions on the line, loss in the line and rise-time of the input signal, and incorporates different design variables into a common design tool. An efficient way to trade-off between the signal rise-time and ringing is discussed.

The objective of transmission line termination is presented as a constrained optimization problem, and using moment models for transmission lines, the *exact* moments of the distributed system can be efficiently evaluated as part of the optimization tool. Several examples are presented to demonstrate the effectiveness of our metric and the results obtained.

References

[1] H. B. Bakoglu, *Circuits, Interconnections, and Packaging for VLSI*. Addison-Wesley Publishing Company, 1990.

[2] W. R. Blood, *MECL System Design Handbook*, Motorola Inc., 1988.

[3] J.R. Brews, "Overshoot-Controlled RLC Interconnections," *IEEE Trans. on Electron Devices*, vol. 38, no. 1, Jan. 1991.

[4] H. Cramér, *Mathematical Methods of Statistics*. Princeton University Press, 1946

[5] R.C. Frye and H.Z. Chen, "Optimal Self-Damped Lossy Transmission Line Interconnections for Multichip Modules," *IEEE Trans. on Circuits and Systems - II: Analog and Digital Signal Processing*, vol. 39, no. 11, Nov. 1992.

[6] P. E. Gill, W. Murray and M.H. Wright, *Practical Optimization*. Academic Press, 1981.

[7] Rohini Gupta and L.T. Pillage, "OTTER: Optimal Termination of Transmission Lines Excluding Radiation," in *Proc. of the 31st ACM/IEEE Design Automation Conf.*, Jun. 1994.

[8] Rohini Gupta, "Synthesis of High-Speed VLSI Interconnects," Ph.D. dissertation, *The University of Texas at Austin*, Aug. 1995.

[9] R. Gupta, J. Willis and L. T. Pillage, "Low Power Design of Off-Chip Drivers and Transmission Lines: A Branch and Bound Approach," to appear in the *Int'l J. of High-Speed Electronics and Systems*, Jan. 1996.

[10] The Authors. In preparation.

[11] B. Krauter, R. Gupta, J. Willis and L. Pileggi, "Transmission line Synthesis," in *Proc. of the 32nd ACM/IEEE Design Automation Conf.*, Jun. 1995, pp. 358-363.

[12] D. G. Luenberger, *Linear and Nonlinear Programming*. Addison-Wesley Publishing Company, 2nd Edition, 1984.

[13] S. Mehrotra, P Franzon, M. Steer, "Performance Driven Global Routing and Wiring Rule Generation for High Speed PCBs and MCMs," in *Proc. of the 32nd ACM/IEEE Design Automation Conf.*, Jun. 1995, pp. 381-387.

[14] L.T. Pillage, R.A. Rohrer and C. Visweswariah, *Electronic Circuit and System Simulation Methods*. McGraw-Hill Inc., 1995.

[15] S. Voranantakul and J.L. Prince, "Efficient Computation of Signal Propagation Delay with Overshoot- and Undershoot Control in VLSI Interconnections," in *SRC Journal Preprint*, SRC Pub. C92603, Oct. 1992.

[16] N.N. Rao, *Elements of Engineering Electromagnetics*. Prentice Hall 1991.

[17] Yo Sugiuchi, Barry Katz and Ronald A. Rohrer, "Interconnect Optimization using Asymptotic Waveform Evaluation(AWE)," in *IEEE Multi-Chip Module Conf.*, Feb. 1994.

[18] David Tuckerman, Tutorial, *IEEE Multi-Chip Module Conference, Feb. 1994*.

[19] M. Sriram and S.M. Kang, "Performance Driven MCM Routing Using a Second Order RLC Tree Delay Model," in *Proc. of the 1993 Int'l Conf. on Wafer Scale Integration*, 1993, pp. 262-267.

[20] Q.J. Yu and E.S. Kuh, "Moment Models of General Transmission Lines with Application to MCM Interconnect Analysis," in *Proc. IEEE Multi-Chip Module Conf.*, Feb. 1995.

[21] D. Zhou, S. Su, F Tsui, D.S. Gao and J.S. Cong, "A Simplified Synthesis of Transmission Lines with a Tree Structure," *Int'l J. of Analog Integrated Circuits and Signal Processing*, Jan. 1994.